

# Enhancing Dynamic Range of Sub-Quantum-Limit Measurements via Quantum Deamplification

Qi Liu,<sup>1,\*</sup> Ming Xue,<sup>2,\*</sup> Xinwei Li,<sup>3</sup> Denis V. Vasilyev,<sup>4</sup> Ling-Na Wu,<sup>5,†</sup> and Vladan Vuletić<sup>1</sup>

<sup>1</sup>*Department of Physics, MIT-Harvard Center for Ultracold Atoms and Research Laboratory of Electronics, Massachusetts Institute of Technology, Cambridge, Massachusetts 02139, USA*

<sup>2</sup>*Department of Physics & Key Laboratory of Aerospace Information Materials and Physics, Nanjing University of Aeronautics and Astronautics, Nanjing 211106, China*

<sup>3</sup>*Beijing Academy of Quantum Information Sciences, Xibeiwang East Road, Beijing 100193, China*

<sup>4</sup>*Institute for Theoretical Physics, University of Innsbruck, 6020 Innsbruck, Austria*

<sup>5</sup>*Center for Theoretical Physics & School of Physics and Optoelectronic Engineering, Hainan University, Haikou 570228, China*

(Dated: January 7, 2025)

Balancing high sensitivity with a broad dynamic range is a fundamental challenge in measurement science, as improving one often compromises the other. While traditional quantum metrology has prioritized enhancing local sensitivity, a large dynamic range is crucial for applications such as atomic clocks, where extended phase interrogation times contribute to wider phase range. In this Letter, we introduce a novel quantum deamplification mechanism that extends dynamic range at a minimal cost of sensitivity. Our approach uses two sequential spin-squeezing operations to generate and detect an entangled probe state, respectively. We demonstrate that the optimal quantum interferometer limit can be approached through two-axis counter-twisting dynamics. Further expansion of dynamic range is possible by using sequential quantum deamplification interspersed with phase encoding processes. Additionally, we show that robustness against detection noise can be enhanced by a hybrid sensing scheme that combines quantum deamplification with quantum amplification. Our protocol is within the reach of state-of-the-art atomic-molecular-optical platforms, offering a scalable, noise-resilient pathway for entanglement-enhanced metrology.

*Introduction.*— In the field of precision measurement, achieving high sensitivity to the signal of interest across a broad measurement range is a key goal [1–3]. Considerable advancements have been made in surpassing the standard quantum limit (SQL)—the best phase sensitivity achievable with uncorrelated particles—by leveraging entangled probe states, including squeezed states [4–18], Dicke states [19–23], and Schrödinger-cat-like states [24–29]. However, the enhanced sensitivity obtained in this way is usually confined to a narrow phase range [30–32]. Moreover, the detection of entangled states is susceptible to technical noise, which diminishes the theoretical metrological benefits promised by entanglement [33, 34]. To address the latter challenge, quantum amplification (QA) techniques [35–41] have been developed. These methods typically amplify the signal through squeezing-unsqueezing protocols [14, 42–45]. The introduction of unsqueezing, however, comes with the trade-off of a limited phase range within which beyond-SQL sensitivity can be achieved [14, 46].

While the emphasis has predominantly been on boosting local sensitivity, the demand for a broad measurement range in practical applications is equally important and warrants greater attention. In the scenario of atomic clocks [47], a broader measurement range enables longer phase interrogation times, which can reduce frequency instability even if local sensitivity is slightly compromised. Previous studies have shown that by using auxiliary interferometers, one can enhance the *dynamic range*, within which the phase can be extracted from the measurement unambiguously. For instance, employing dual-quadrature measurement with two ensembles doubles dynamic range [48, 49]. Even greater enhancement in dynamic range is possible through the use of multiple ensembles with different interrogation phases [50–54]. By in-

tegrating these techniques with entangled states, it is possible to achieve beyond-SQL phase sensitivity across an extended phase range [25, 26, 49, 55–57]. The ultimate goal is to optimize both estimation precision and dynamic range by leveraging quantum resources native to the experimental platform. This can be achieved via quantum variational optimization, which designs quantum circuits generating optimal input states and measurements that minimize the Bayesian mean squared error for a given prior distribution of a parameter [30, 58]. Experimental implementations [59] of such circuits approach the performance of an optimal quantum interferometer (OQI) [60] but face increasing circuit complexity as system size grows. The challenge lies in identifying quantum sensing protocols and resources that enable simple, robust circuits capable of nearing OQI performance despite experimental imperfections.

In this paper, we introduce a novel mechanism that leverages *quantum deamplification* (QD) to extend dynamic range using a single ensemble in the presence of detection noise. Unlike the QA protocols [35, 42, 45], our method employs two sequential squeezing stages to deamplify the encoded phase at a minimal cost of local sensitivity, thereby achieving a broader dynamic range. We demonstrate this mechanism by using a generalized Ramsey interferometer based on two-axis counter-twisting (TACT) interaction [4, 61, 62], which is both efficient in generating spin squeezing and particularly elegant for illustrating the core idea of our approach. This method approaches the OQI limit in sensing performance using only one TACT gate each for state preparation and measurement. Furthermore, interspersing phase encoding with TACT squeezing—progressively deamplifying the signal—expands dynamic range further, albeit with reduced local sensitivity, bringing the overall single-shot sensing performance

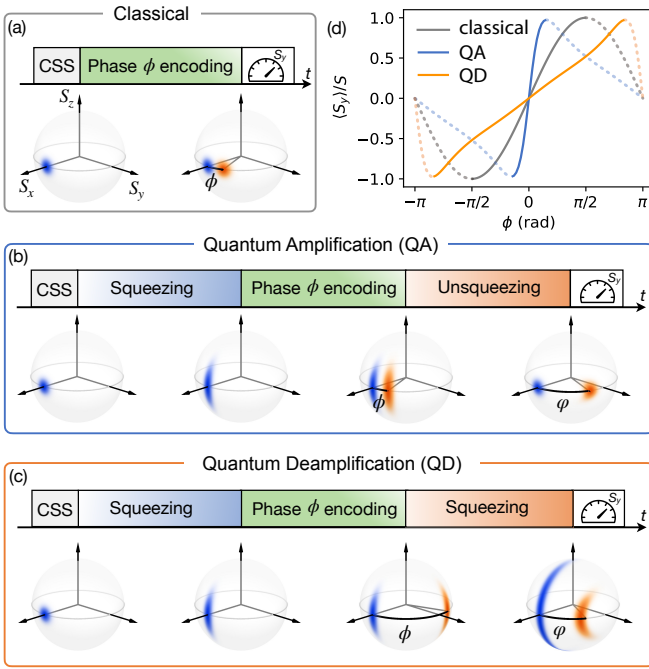


Figure 1. The interferometry time sequence and corresponding Husimi representations of states for (a) classical probe, (b) quantum amplification (QA), and (c) quantum deamplification (QD). The blue (orange) shading denotes the state without (with) phase  $\phi$  encoding. (d) Normalized spin observable  $\langle S_y \rangle / S$  as a function of phase  $\phi$ . The coherent spin state provides a dynamic range around  $[-\pi/2, \pi/2]$  (grey solid line), within which the phase can be distinguished unambiguously. QA narrows the dynamic range (blue solid line), while QD extends the dynamic range to nearly  $[-\pi, \pi]$  (orange solid line). Dashed lines denote the intervals where phase slip error occurs.

closer to the OQI limit. To enhance noise robustness, we propose a hybrid sensing protocol combining QD, QA, and adaptive one-way local operations and classical communication measurements [63], enabling high-sensitivity phase estimation over a wide dynamic range despite experimental imperfections.

*Quantum (de)amplification.*— We consider estimation of the phase  $\phi$  in an atomic interferometer consisting of  $N$  identical two-level atoms. For a classical probe in the coherent spin state (CSS), as shown in Fig. 1(a), the measurement precision is inherently bounded by the SQL,  $1/\sqrt{N}$ . The ambiguity-free dynamic range is confined to  $[-\pi/2, \pi/2]$ , within which the observable varies monotonically with  $\phi$  [grey solid curve in Fig. 1(d)]. This limitation arises because  $\phi$  and  $\pm\pi - \phi$  yield the same measurement outcome, leading to significant bias error when the phase is out of the dynamic range. In the QA protocol [Fig. 1(b)], a squeezing-encoding-unsqueezing sequence amplifies the encoded signal. Since the amplified phase  $\varphi$  can only be distinctly resolved within the range  $[-\pi/2, \pi/2]$ , the estimation range of encoded phase  $\phi$  ( $\leq \varphi$ ) is further limited. This is illustrated by the blue solid curve in Fig. 1(d), which shows a steeper gradient near small phases and a reduced dynamic range. In contrast, we propose introducing a squeezing

instead of unsqueezing process before measurement, which deamplifies the signal  $\phi$  [see Fig. 1(c) for the QD sequence]. Given that the sensing range of the deamplified phase  $\varphi$  is confined to the classical boundary of  $[-\pi/2, \pi/2]$ , the ambiguity-free dynamic range of the encoded phase  $\phi$  ( $\geq \varphi$ ) is extended beyond this interval, as shown by the orange solid curve in Fig. 1(d).

*QD-based sensing with TACT interactions.*— Building on the above discussion, we now delve into a more detailed examination of our proposal. We employ the TACT squeezing model [4], governed by the Hamiltonian  $\hat{H}_{\text{TACT}} = \chi(\hat{S}_y\hat{S}_z + \hat{S}_z\hat{S}_y)$  with interaction strength  $\chi$ , where  $\hat{S}_{x,y,z} = \sum_{k=1}^N \hat{\sigma}_{x,y,z}^{(k)}/2$  are the collective spin operators and  $\hat{\sigma}_{x,y,z}^{(k)}$  the Pauli operators for the  $k$ -th atom. The structure of our QD-based quantum interferometer is shown in Fig. 2(a). It begins with a CSS as the initial state  $|\Psi_0\rangle$ , followed by the application of the TACT interaction twice [also cf. Fig. 1(c)]. The first instance of TACT interaction precedes the phase encoding process, serving to prepare an entangled probe state, while the second application takes place after phase encoding, facilitating nonlinear readout. The encoded phase is inferred from the collective spin  $\hat{S}_y$  through projective measurements.

The phase estimation accuracy is characterized by the mean squared error (MSE) with respect to the actual phase  $\phi$ ,  $\epsilon(\phi) = \sum_m [\phi - \phi_{\text{est}}(m)]^2 p(m|\phi)$ , where  $p(m|\phi)$  denotes the conditional probability of measurement outcome  $m$ , and is given by  $p(m|\phi) = |\langle m|\hat{U}(t_2)e^{-i\phi\hat{S}_z}\hat{U}(t_1)|\Psi_0\rangle|^2$ , with  $|m\rangle \equiv |S = N/2, S_y = m\rangle$  being the eigenstate of  $\hat{S}_y$  with eigenvalue  $m$ . Here,  $\hat{U}(t) = e^{-i\hat{H}_{\text{TACT}}t}$ , and  $t_1, t_2$  represent the evolution time parameters for the two TACT segments. The optimal values of  $t_1$  and  $t_2$  are to be found through optimization. We assume a linear estimator  $\phi_{\text{est}}(m) = am$ , and the optimal  $a$  is determined from the measurement outcome distribution [58]. Our goal is to achieve optimal sensitivity for phase  $\phi$  in a prior phase range  $\delta\phi$ . Assuming a Gaussian prior phase distribution centered at zero,  $\mathcal{P}_{\delta\phi}(\phi) = \exp[-\phi^2/(\sqrt{2}\delta\phi)^2]/\sqrt{2\pi}(\delta\phi)^2$ , we minimize the MSE averaged over the prior distribution, defining the Bayesian mean squared error (BMSE):  $(\Delta\phi)^2 = \int d\phi \epsilon(\phi)\mathcal{P}_{\delta\phi}(\phi)$ .

Figure 2(b) and (c) showcase the performance of our QD-based sensor, compared to the OQI, classical, and QA-based sensor. In Fig. 2(b), we depict the ratio of posterior uncertainty  $\Delta\phi$  to the prior uncertainty  $\delta\phi$ , minimized individually at each  $\delta\phi$  for QD sensor and OQI. This quantity is related to frequency stability in atomic clock, characterized by the Allan deviation [59, 64]. A smaller value of  $\Delta\phi/\delta\phi$  indicates a lower phase estimation error (smaller  $\Delta\phi$ ) over a broader phase range (larger  $\delta\phi$ ). For all cases,  $\Delta\phi/\delta\phi$  initially declines as  $\delta\phi$  grows and then starts to rise due to increased probability of phase slip error [30, 34, 58]. When compared to the classical Ramsey interferometer (black line, CSS), the QA-based sensor (blue line, QA) enhances sensitivity only at small  $\delta\phi$  values, due to reduced dynamic range caused by signal amplification. The QD-based sensor (orange curve), involving a squeezing-encoding-squeezing sequence, signif-

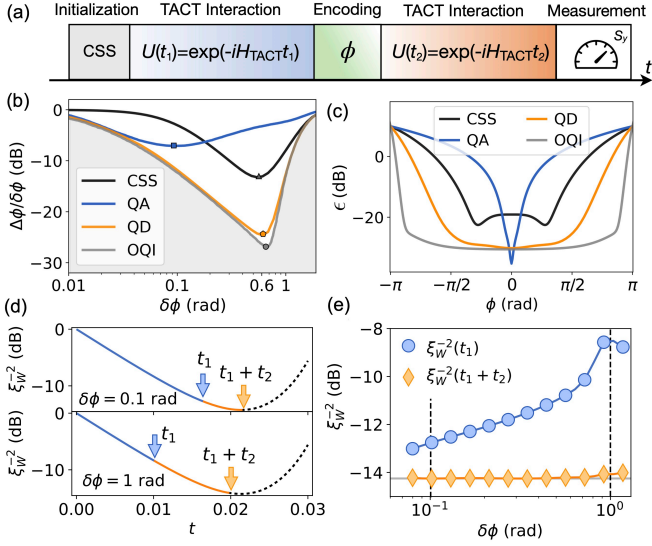


Figure 2. (a) QD-based sensing with TACT interactions. The protocol sequence starts from a coherent spin state (CSS) along  $x$  direction which evolves to a spin squeezed state under TACT evolution  $U(t_1)$ . After a phase ( $\phi$ ) encoding operation,  $U(t_2)$  deamplifies the signal before the final measurement of  $\hat{S}_y$ . (b) The sensor performances, characterized by  $\Delta\phi/\delta\phi$ , of OQI (grey line) and QD sensors (orange line) are optimized at each  $\delta\phi$ , while QA-based sensor (blue line) with TACT interaction uses a fixed interacting time ( $t_1 = -t_2 = 0.022$ ) corresponding to the optimal spin squeezing. The grey shading denotes the inaccessible regime with one-time phase encoding, bounded by the OQI limit. Markers highlight the best performance (minima) at the turning point. (c) MSE of the sensing schemes, evaluated at  $\delta\phi$  and TACT squeezing times corresponding to the minima (markers) of  $\Delta\phi/\delta\phi$  in (b). (d) TACT-interacting times  $t_1$  (blue) and  $t_1+t_2$  (orange) and their corresponding Wineland parameters ( $\xi_W^{-2}$ ) evolution, for two selected  $\delta\phi$  marked by dashed vertical lines in (e). (e) Wineland parameters for the  $\delta\phi$ -dependent optimal probe (blue circles) and final state (orange diamonds) in the QD scheme. The horizontal grey line marks the optimal spin squeezing obtainable with TACT interaction. All calculations in this paper assume  $N = 100$  and  $\chi = 1$ .

icantly enhances the precision of phase estimation at large  $\delta\phi$ . Notably, its performance nearly approaches the theoretical limit given by the OQI (grey curve) with the optimal probe state and measurement [60]. Figure 2(c) displays the MSE as a function of the phase  $\phi$ . The prior uncertainties  $\delta\phi$  and TACT squeezing times are selected to achieve the minimal  $\Delta\phi/\delta\phi$  as indicated by the markers in panel (b). It is evident that the QA-based sensor (blue curve) outperforms the classical interferometer (black curve) only for small values of  $\phi$ . In contrast, the QD-based sensing protocol (orange curve) diminishes the error throughout the entire range of  $[-\pi, \pi]$ .

The superior performance of the QD-based sensing protocol can be credited to the aforementioned squeezing-squeezing mechanism which allows for an extended dynamic range. This is clearly demonstrated in Fig. 2(d), which shows the evolution of the system's squeezing degree for two distinct  $\delta\phi$ . The squeezing degree is quantified by the

Wineland parameter [65, 66],  $\xi_W^{-2} = N\Delta^2\hat{S}_{\perp,\min}/|\langle\hat{\mathbf{S}}\rangle|^2$ , where  $\Delta^2\hat{S}_{\perp,\min}$  denotes the minimal spin fluctuation on the plane perpendicular to the mean spin direction and the collective spin vector  $\hat{\mathbf{S}} = (\hat{S}_x, \hat{S}_y, \hat{S}_z)$ . Figure 2(d) reveals a sequential squeezing process, where the initial squeezing (blue segment) creates a spin squeezed state as a probe, while the subsequent squeezing (orange segment), leads to signal deamplification, thereby enhancing the dynamic range. An overview of the Wineland parameter as a function of  $\delta\phi$  is shown in Fig. 2(e). One can see that the squeezing of the probe state (blue) is always less pronounced than that of the final state (orange). Particularly, the final state is close to the optimal squeezed state. In other words, the journey to the optimal squeezed state is divided into two segments, one for state preparation and the other for signal deamplification. The timing for phase encoding, nestled between these two processes, depends on the prior phase uncertainty: for a broader prior distribution (larger  $\delta\phi$ ), phase encoding should occur earlier to maximize the signal deamplification effect, as shown in Fig. 2(d). Furthermore, we claim that the QD mechanism based on sequential squeezing is not limited to the TACT model and can be generalized to other interactions [67].

*Sequential QD interspersed with phase encoding.*—Given the cyclical nature of phase encoding via unitary  $e^{-i\phi\hat{S}_z}$ —where  $\phi$  and  $\phi + 2\pi$  are indistinguishable—the maximum dynamic range of the aforementioned methodologies is inherently restricted to the interval  $[-\pi, \pi]$ . To surmount this limitation, we propose enhancing phase encoding with sequential QD [67]. As illustrated in Fig. 3(a), this approach involves the iterative application of spin squeezing interspersed

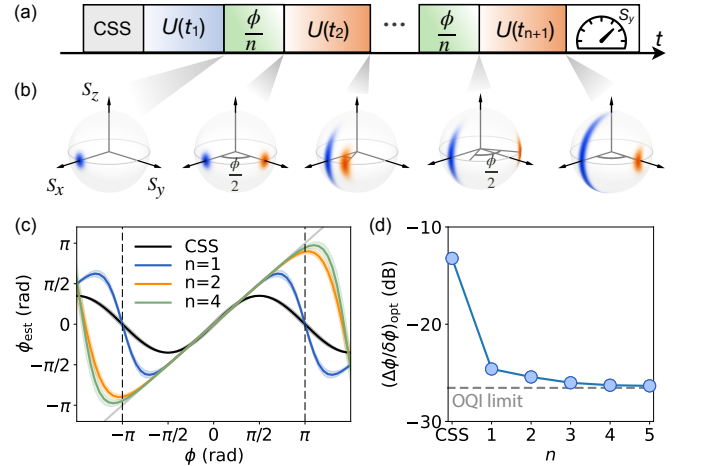


Figure 3. (a) Schematics of the sequential QD interspersed with phase encoding. (b) Evolution of quantum state on the Bloch spheres for  $n = 2$ . Squeezing times are  $t_1 = 0.0022$ ,  $t_2 = 0.014$ , and  $t_3 = 0.0061$ , with a total time cost close to the optimal squeezing time in Fig. 2(d). (c) Estimated phase  $\phi_{\text{est}}$  as a function of the real phase  $\phi$ . The shading represents the square root of the MSE. The grey solid line denotes the unbiased estimation with  $\phi_{\text{est}} = \phi$ . Black dashed vertical lines label  $\phi = \pm\pi$ . (d) Optimal  $\Delta\phi/\delta\phi_{\text{opt}}$  as a function of  $n$ . The OQI limit is illustrated by the grey dashed line.

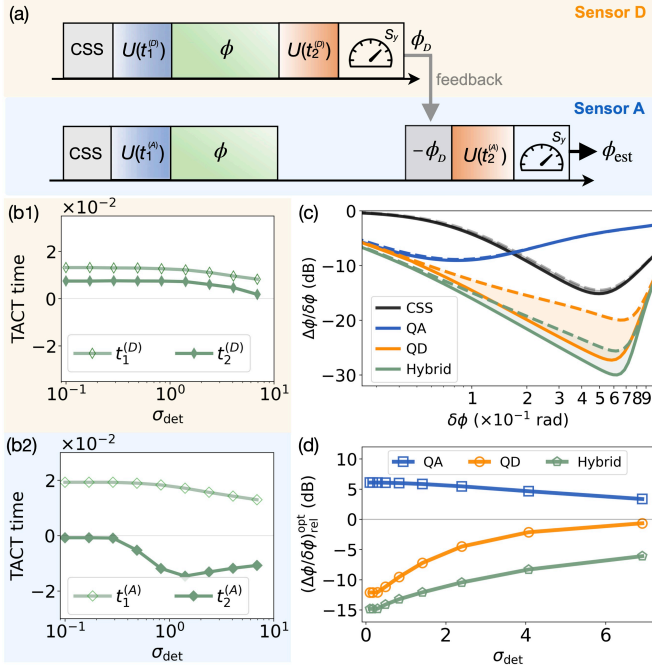


Figure 4. Hybrid sensing with adaptive measurement. (a) Two sensors are conjointly used for measuring the phase of LO. The phase estimated from the sensor D is subtracted from the phase encoded on sensor A. (b1-b2) The optimal TACT-interacting times for the two sensors as a function of detection noise. Negative time in (b2) corresponds to a sign-flip of  $\chi$ . (c) Optimized  $\Delta\phi/\delta\phi$  for various sensing schemes. The solid (dashed) curves denote the results in the absence (presence, with  $\sigma_{\text{det}} = 2$ ) of detection noise. (d) The minimal phase estimation error with respect to the classical sensor,  $(\Delta\phi/\delta\phi)_{\text{rel}}^{\text{opt}} \equiv (\Delta\phi/\delta\phi)^{\text{opt}}/(\Delta\phi/\delta\phi)_{\text{CSS}}^{\text{opt}}$ , as a function of detection noise  $\sigma_{\text{det}}$ .

with phase encoding. In the limit of infinite iterations, it approaches concurrent entanglement generation and phase interrogation, as previously used to unify state preparation and phase encoding [68, 69]. This methodical layering of phase encoding and TACT interaction serves to deamplify the signal progressively [Fig. 3(b)], thereby extending the dynamic range beyond  $[-\pi, \pi]$ . In Fig. 3(c), the estimated phase  $\phi_{\text{est}}$  is depicted as a function of the encoded phase  $\phi$ , across various iterations  $n$ . The ideal estimation is unbiased, aligning  $\phi_{\text{est}}$  with  $\phi$ , as indicated by the grey solid line. One can see that with each additional layer of phase encoding, the unambiguous phase estimation range is enhanced. The sequential QD also brings the benefit of reducing BMSE as shown in Fig. 3(d), which converges to the OQI limit with increasing  $n$ .

*Hybrid sensing with adaptive measurement.*— In the absence of detection noise, the QD sensor is capable of approaching the OQI performance, providing a near-optimal balance between the local sensitivity and phase sensing range. However, the QD sequence ends up with a highly squeezed state before measurement, which renders the metrological performance susceptible to detection noise. This challenge also exists in the circuit optimization for a generalized Ramsey in-

terferometers based on one-axis twirling [30, 58], and poses one practical limitation of the latter in large systems. In contrast, QA sensor exhibits strong resilience to detection noise, though this robustness comes at the expense of a narrower dynamic range. Here we study a *hybrid sensing* scheme [64] to harness the complementary strengths of these two sensors in a synergistic manner. The QD sensor, with its ability to offer a broad dynamic range is utilized for the initial phase detection. It allows for the sensing process to effectively handle a variety of phase shifts, although the sensitivity would be compromised by detection noise. To address this, we then employ the QA sensor with an *adaptive* measurement to refine the phase estimation, improving the system’s resilience to noise and reducing the phase estimation error.

To validate our idea numerically, we design a hybrid system comprising two TACT-based sensors interrogated with the same local oscillator (LO), as shown in Fig. 4(a). The first sensor (D) provides an initial estimate of the LO phase  $\phi$ , called  $\phi_D$ . This phase estimate is fed back to the second sensor (A) by adjusting the control pulse phase, effectively adding  $-\phi_D$  to the interrogation phase  $\phi$ . Finally, by analyzing its output to get  $\phi_A$ , we estimate the phase  $\phi$  as  $\phi_{\text{est}} = \phi_D + \phi_A$ .

We optimize the TACT-interacting times at two stages—before and after the phase encoding—in both sensors,  $\{t_1^{(D)}, t_2^{(D)}, t_1^{(A)}, t_2^{(A)}\}$ , with the goal of minimizing the BMSE in the presence of detection noise  $\sigma_{\text{det}}$  [70]. The results, depicted in Fig. 4(b), illustrate how these interaction times vary with the level of detection noise. The interaction times for the first sensor are both positive ( $t_{1,2}^{(D)} > 0$ ), signifying its role as a QD sensor with a sequential squeezing process. On the other hand, the second sensor exhibits a positive interaction time prior to phase encoding ( $t_1^{(A)} > 0$ ) and a negative interaction time post phase encoding ( $t_2^{(A)} < 0$ ), which is indicative of a QA sensor with a squeezing-unsqueezing mechanism.

In Fig. 4(c), we compare the BMSE of the hybrid sensor with several individual sensing schemes. To guarantee a fair comparison, we employ the same total number of particles in all the schemes. The solid (dashed) curves denote the results in the absence (presence, with  $\sigma_{\text{det}} = 2$ ) of detection noise. Among the individual sensing schemes (either split into two independent sensors of  $N$  atoms each or measured independently twice with  $N$  atoms [67]), the QA sensor (blue curves) exhibits strong resilience to detection noise (highlighted by the shading area), while it falls short in BMSE. In contrast, the QD sensor (orange curves) provides a small phase estimation error over a broad range of  $\delta\phi$ , but is highly susceptible to detection noise. The hybrid sensor (green curves), which combines the strengths of both QD and QA sensors, demonstrates robustness against detection noise and maintains low phase estimation error across a broad range of phase. Figure 4(d) further highlights the resilience difference between the sensors. One can see that the hybrid sensor (green curve) consistently outperforms the other sensors across all levels of detection noise, and its performance degrades slower with in-

creasing detection noise compared to the individual QD sensor.

*Conclusion*— We introduce a novel QD mechanism to extend the dynamic range of phase measurements through squeezing-encoding-squeezing operations, which is demonstrated by using a TACT-based interferometer. The phase encoded on the squeezed probe state gets deamplified during the second squeezing stage at a minimal cost of local sensitivity, thereby achieving a broader dynamic range and approaching the OQI limit. This scheme is further enhanced by sequential QD interspersed with multiple phase encoding processes. Since the QD sequence ends in a highly squeezed state before measurement, its metrological performance becomes susceptible to detection noise. To address this limitation, we propose a hybrid sensing scheme that combines the advantages of both QD and QA sensors to achieve a precise and robust phase sensing.

Our protocols are accessible with current cold atom and molecule experiments. Recent experiments have successfully demonstrated the mean-field spin dynamics of the TACT model in cavity QED systems [61] and ultracold polar molecules [62], making the observation of spin squeezing highly promising in the near future. Furthermore, the hybrid sensing approach incorporating QA and QD can be extended to generalized Ramsey interferometry with one-axis twisting interactions [4], making it broadly applicable to diverse quantum systems such as Bose-Einstein condensates [14], trapped ions [71], and Rydberg atom arrays [72, 73]. Overall, our method offers a promising advancement in entanglement-enhanced metrology, with the potential to significantly improve applications such as the long-term stability of atomic clocks and other precision measurement systems [74].

*Acknowledgement.* We thank Leon Zaporski, Matthew Radzihovsky, Gustavo Velez, Guo-Qing Wang and Zhi-Yao Hu for helpful discussion. This work is supported by the National Natural Science Foundation of China (No. 12304543) and the Innovation Program for Quantum Science and Technology (No. 2021ZD0302100). L.-N.W. acknowledges support by the Hainan Province Science and Technology Talent Innovation Project (No. KJRC2023L05). D.V.V. acknowledges funding by the Austrian Science Fund (FWF) [10.55776/COE1]. M.X. is also supported by the Jiangsu Province & Longcheng Youth Science and Technology Talent Support Project.

\* These authors contributed equally to this work.

† [lingna.wu@hainanu.edu.cn](mailto:lingna.wu@hainanu.edu.cn)

- [1] C. L. Degen, F. Reinhard, and P. Cappellaro, Quantum sensing, *Rev. Mod. Phys.* **89**, 035002 (2017).
- [2] L. Pezzè, A. Smerzi, M. K. Oberthaler, R. Schmied, and P. Treutlein, Quantum metrology with nonclassical states of atomic ensembles, *Rev. Mod. Phys.* **90**, 035005 (2018).
- [3] J. Huang, M. Zhuang, and C. Lee, Entanglement-enhanced quantum metrology: From standard quantum limit to heisenberg limit, *Applied Physics Reviews* **11**, 031302 (2024).
- [4] M. Kitagawa and M. Ueda, Squeezed spin states, *Phys. Rev. A* **47**, 5138 (1993).
- [5] A. Kuzmich, K. Mølmer, and E. S. Polzik, Spin squeezing in an ensemble of atoms illuminated with squeezed light, *Phys. Rev. Lett.* **79**, 4782 (1997).
- [6] J. Hald, J. L. Sørensen, C. Schori, and E. S. Polzik, Spin squeezed atoms: A macroscopic entangled ensemble created by light, *Phys. Rev. Lett.* **83**, 1319 (1999).
- [7] C. Gross, T. Zibold, E. Nicklas, J. Estève, and M. K. Oberthaler, Nonlinear atom interferometer surpasses classical precision limit, *Nature* **464**, 1165 (2010).
- [8] M. F. Riedel, P. Böhi, Y. Li, T. W. Hänsch, A. Sinatra, and P. Treutlein, Atom-chip-based generation of entanglement for quantum metrology, *Nature* **464**, 1170 (2010).
- [9] L. Pezzè and A. Smerzi, Ultrasensitive two-mode interferometry with single-mode number squeezing, *Phys. Rev. Lett.* **110**, 163604 (2013).
- [10] R. Schmied, J.-D. Bancal, B. Allard, M. Fadel, V. Scarani, P. Treutlein, and N. Sangouard, Bell correlations in a bose-einstein condensate, *Science* **352**, 441 (2016).
- [11] E. S. Polzik and J. Ye, Entanglement and spin squeezing in a network of distant optical lattice clocks, *Phys. Rev. A* **93**, 021404 (2016).
- [12] J. G. Bohnet, B. C. Sawyer, J. W. Britton, M. L. Wall, A. M. Rey, M. Foss-Feig, and J. J. Bollinger, Quantum spin dynamics and entanglement generation with hundreds of trapped ions, *Science* **352**, 1297 (2016).
- [13] S. Colombo, E. Pedrozo-Peñañiel, and V. Vuletić, Entanglement-enhanced optical atomic clocks, *Applied Physics Letters* **121** (2022).
- [14] T.-W. Mao, Q. Liu, X.-W. Li, J.-H. Cao, F. Chen, W.-X. Xu, M. K. Tey, Y.-X. Huang, and L. You, Quantum-enhanced sensing by echoing spin-nematic squeezing in atomic bose-einstein condensate, *Nature Physics* **19**, 1585 (2023).
- [15] G. P. Greve, C. Luo, B. Wu, and J. K. Thompson, Entanglement-enhanced matter-wave interferometry in a high-finesse cavity, *Nature* **610**, 472 (2022).
- [16] D. Ganapathy, W. Jia, M. Nakano, and et al (LIGO O4 Detector Collaboration), Broadband quantum enhancement of the ligo detectors with frequency-dependent squeezing, *Phys. Rev. X* **13**, 041021 (2023).
- [17] W. Jia, V. Xu, K. Kuns, and et al, Squeezing the quantum noise of a gravitational-wave detector below the standard quantum limit, *Science* **385**, 1318 (2024).
- [18] J. M. Robinson, M. Miklos, Y. M. Tso, C. J. Kennedy, T. Bothwell, D. Kedar, J. K. Thompson, and J. Ye, Direct comparison of two spin-squeezed optical clock ensembles at the  $10^{-17}$  level, *Nature Physics* **20**, 208 (2024).
- [19] S. F. Huelga, C. Macchiavello, T. Pellizzari, A. K. Ekert, M. B. Plenio, and J. I. Cirac, Improvement of frequency standards with quantum entanglement, *Phys. Rev. Lett.* **79**, 3865 (1997).
- [20] B. Lücke, M. Scherer, J. Kruse, L. Pezzè, F. Deuretzbacher, P. Hyllus, O. Topic, J. Peise, W. Ertmer, J. Arlt, L. Santos, A. Smerzi, and C. Klempt, Twin matter waves for interferometry beyond the classical limit, *Science* **334**, 773 (2011).
- [21] Z. Zhang and L. M. Duan, Quantum metrology with dicke squeezed states, *New Journal of Physics* **16**, 103037 (2014).
- [22] X.-Y. Luo, Y.-Q. Zou, L.-N. Wu, Q. Liu, M.-F. Han, M. K. Tey, and L. You, Deterministic entanglement generation from driving through quantum phase transitions, *Science* **355**, 620 (2017).
- [23] Y.-Q. Zou, L.-N. Wu, Q. Liu, X.-Y. Luo, S.-F. Guo, J.-H. Cao, M. K. Tey, and L. You, Beating the classical precision limit with

- spin-1 dicke states of more than 10,000 atoms, [Proceedings of the National Academy of Sciences](#) **115**, 6381 (2018).
- [24] T. Chalopin, C. Bouazza, A. Evrard, V. Makhalov, D. Dreon, J. Dalibard, L. A. Sidorenkov, and S. Nascimbene, Quantum-enhanced sensing using non-classical spin states of a highly magnetic atom, [Nature Communications](#) **9**, 4955 (2018).
- [25] A. Cao, W. J. Eckner, T. Lukin Yelin, A. W. Young, S. Jandura, L. Yan, K. Kim, G. Pupillo, J. Ye, N. Darkwah Oppong, *et al.*, Multi-qubit gates and schrödinger cat states in an optical clock, [Nature](#) **634**, 315 (2024).
- [26] R. Finkelstein, R. B.-S. Tsai, X. Sun, P. Scholl, S. Direkci, T. Gefen, J. Choi, A. L. Shaw, and M. Endres, Universal quantum operations and ancilla-based read-out for tweezer clocks, [Nature](#) **634**, 321 (2024).
- [27] T. Kielinski, P. O. Schmidt, and K. Hammerer, GHZ protocols enhance frequency metrology despite spontaneous decay, [Science Advances](#) **10**, eadr1439 (2024).
- [28] Y. A. Yang, W. T. Luo, J. L. Zhang, S. Z. Wang, C.-L. Zou, T. Xia, and Z. T. Lu, Minute-scale schrödinger-cat state of spin-5/2 atoms, [Nature Photonics](#) **10.1038/s41566-024-01555-3** (2024).
- [29] X. Zhang, Z. Hu, and Y.-C. Liu, Fast generation of ghz-like states using collective-spin XYZ model, [Phys. Rev. Lett.](#) **132**, 113402 (2024).
- [30] R. Kaubruegger, D. V. Vasilyev, M. Schulte, K. Hammerer, and P. Zoller, Quantum variational optimization of ramsey interferometry and atomic clocks, [Phys. Rev. X](#) **11**, 041045 (2021).
- [31] R. Kaubruegger, A. Shankar, D. V. Vasilyev, and P. Zoller, Optimal and variational multiparameter quantum metrology and vector-field sensing, [PRX Quantum](#) **4**, 020333 (2023).
- [32] D. V. Vasilyev, A. Shankar, R. Kaubruegger, and P. Zoller, [Optimal multiparameter metrology: The quantum compass solution](#) (2024), [arXiv:2404.14194 \[quant-ph\]](#).
- [33] A. André, A. S. Sørensen, and M. D. Lukin, Stability of atomic clocks based on entangled atoms, [Phys. Rev. Lett.](#) **92**, 230801 (2004).
- [34] M. Schulte, C. Lisdat, P. O. Schmidt, U. Sterr, and K. Hammerer, Prospects and challenges for squeezing-enhanced optical atomic clocks, [Nature Communications](#) **11**, 5955 (2020).
- [35] E. Davis, G. Bentsen, and M. Schleier-Smith, Approaching the heisenberg limit without single-particle detection, [Phys. Rev. Lett.](#) **116**, 053601 (2016).
- [36] S. P. Nolan, S. S. Szigeti, and S. A. Haine, Optimal and robust quantum metrology using interaction-based readouts, [Phys. Rev. Lett.](#) **119**, 193601 (2017).
- [37] S. A. Haine, Using interaction-based readouts to approach the ultimate limit of detection-noise robustness for quantum-enhanced metrology in collective spin systems, [Phys. Rev. A](#) **98**, 030303 (2018).
- [38] Q. Liu, L.-N. Wu, J.-H. Cao, T.-W. Mao, X.-W. Li, S.-F. Guo, M. K. Tey, and L. You, Nonlinear interferometry beyond classical limit enabled by cyclic dynamics, [Nature Physics](#) **18**, 167 (2022).
- [39] Q. Liu, T.-W. Mao, M. Xue, L.-N. Wu, and L. You, Cyclic nonlinear interferometry with entangled non-gaussian spin states, [Phys. Rev. A](#) **107**, 052613 (2023).
- [40] Z. Hu, Q. Li, X. Zhang, L.-G. Huang, H.-b. Zhang, and Y.-C. Liu, Spin squeezing with arbitrary quadratic collective-spin interactions, [Phys. Rev. A](#) **108**, 023722 (2023).
- [41] Z. Hu, Q. Li, X. Zhang, H.-b. Zhang, L.-G. Huang, and Y.-C. Liu, Nonlinear time-reversal interferometry with arbitrary quadratic collective-spin interaction, [Chinese Physics B](#) (2023).
- [42] O. Hosten, R. Krishnakumar, N. J. Engelsen, and M. A. Kasevich, Quantum phase magnification, [Science](#) **352**, 1552 (2016).
- [43] D. Linnemann, H. Strobel, W. Muessel, J. Schulz, R. J. Lewis-Swan, K. V. Kheruntsyan, and M. K. Oberthaler, Quantum-enhanced sensing based on time reversal of nonlinear dynamics, [Phys. Rev. Lett.](#) **117**, 013001 (2016).
- [44] S. C. Burd, R. Srinivas, J. J. Bollinger, A. C. Wilson, D. J. Wineland, D. Leibfried, D. H. Slichter, and D. T. C. Allcock, Quantum amplification of mechanical oscillator motion, [Science](#) **364**, 1163 (2019).
- [45] S. Colombo, E. Pedrozo-Penafiel, A. F. Adiyatullin, Z. Li, E. Mendez, C. Shu, and V. Vuletić, Time-reversal-based quantum metrology with many-body entangled states, [Nature Physics](#) **18**, 925 (2022).
- [46] S. Colombo, E. Pedrozo-Penafiel, and V. Vuletić, Entanglement-enhanced optical atomic clocks, [Applied Physics Letters](#) **121**, 210502 (2022).
- [47] A. D. Ludlow, M. M. Boyd, J. Ye, E. Peik, and P. O. Schmidt, Optical atomic clocks, [Rev. Mod. Phys.](#) **87**, 637 (2015).
- [48] T. Rosenband and D. R. Leibbrandt, [Exponential scaling of clock stability with atom number](#) (2013), [arXiv:1303.6357 \[quant-ph\]](#).
- [49] W. Li, S. Wu, A. Smerzi, and L. Pezzè, Improved absolute clock stability by the joint interrogation of two atomic ensembles, [Phys. Rev. A](#) **105**, 053116 (2022).
- [50] D. B. Hume and D. R. Leibbrandt, Probing beyond the laser coherence time in optical clock comparisons, [Phys. Rev. A](#) **93**, 032138 (2016).
- [51] J. Borregaard and A. S. Sørensen, Near-heisenberg-limited atomic clocks in the presence of decoherence, [Phys. Rev. Lett.](#) **111**, 090801 (2013).
- [52] D. Yankelev, C. Avinadav, N. Davidson, and O. Firstenberg, Atom interferometry with thousand-fold increase in dynamic range, [Science Advances](#) **6**, eabd0650 (2020).
- [53] A. L. Shaw, R. Finkelstein, R. B.-S. Tsai, P. Scholl, T. H. Yoon, J. Choi, and M. Endres, Multi-ensemble metrology by programming local rotations with atom movements, [Nature Physics](#) **20**, 195 (2024).
- [54] X. Zheng, J. Dolde, and S. Kolkowitz, Reducing the instability of an optical lattice clock using multiple atomic ensembles, [Phys. Rev. X](#) **14**, 011006 (2024).
- [55] S. Direkci, R. Finkelstein, M. Endres, and T. Gefen, Heisenberg-limited bayesian phase estimation with low-depth digital quantum circuits, [arXiv preprint arXiv:2407.06006](#) (2024).
- [56] L.-Z. Liu, Y.-Y. Fei, Y. Mao, Y. Hu, R. Zhang, X.-F. Yin, X. Jiang, L. Li, N.-L. Liu, F. Xu, Y.-A. Chen, and J.-W. Pan, Full-period quantum phase estimation, [Phys. Rev. Lett.](#) **130**, 120802 (2023).
- [57] J. Zhou, J. Huang, J. Wei, C. Han, and C. Lee, [High-dynamic-range atomic clocks with dual heisenberg-limited precision scaling](#) (2024), [arXiv:2411.14944 \[quant-ph\]](#).
- [58] T. G. Thurtell and A. Miyake, Optimizing one-axis twists for variational bayesian quantum metrology, [Phys. Rev. Res.](#) **6**, 023179 (2024).
- [59] C. D. Marciniak, T. Feldker, I. Pogorelov, R. Kaubruegger, D. V. Vasilyev, R. van Bijnen, P. Schindler, P. Zoller, R. Blatt, and T. Monz, Optimal metrology with programmable quantum sensors, [Nature](#) **603**, 604 (2022).
- [60] K. Macieszczak, M. Fraas, and R. Demkowicz-Dobrzański, Bayesian quantum frequency estimation in presence of collective dephasing, [New Journal of Physics](#) **16**, 113002 (2014).
- [61] C. Luo, H. Zhang, A. Chu, C. Maruko, A. M. Rey, and J. K. Thompson, [Hamiltonian engineering of collective xyz spin models in an optical cavity](#) (2024), [arXiv:2402.19429 \[quant-ph\]](#).

- ph].
- [62] C. Miller, A. N. Carroll, J. Lin, H. Hirzler, H. Gao, H. Zhou, M. D. Lukin, and J. Ye, Two-axis twisting using floquet-engineered xyz spin models with polar molecules, *Nature* **633**, 332 (2024).
- [63] E. Chitambar, D. Leung, L. Mančinska, M. Ozols, and A. Winter, Everything you always wanted to know about LOCC (but were afraid to ask), *Communications in Mathematical Physics* **328**, 303 (2014).
- [64] L. Pezzè and A. Smerzi, Heisenberg-limited noisy atomic clock using a hybrid coherent and squeezed state protocol, *Phys. Rev. Lett.* **125**, 210503 (2020).
- [65] D. J. Wineland, J. J. Bollinger, W. M. Itano, F. L. Moore, and D. J. Heinzen, Spin squeezing and reduced quantum noise in spectroscopy, *Phys. Rev. A* **46**, R6797 (1992).
- [66] D. J. Wineland, J. J. Bollinger, W. M. Itano, and D. J. Heinzen, Squeezed atomic states and projection noise in spectroscopy, *Phys. Rev. A* **50**, 67 (1994).
- [67] The supplementary material includes: (1) a discussion on the generality of the QD mechanism, (2) additional details and discussions on the sequential QD scheme, and (3) specifics on the variational parameter optimization in a multi-ensemble system, (4) similarities between the TACT-based QD sensor and OQI.
- [68] S. A. Haine and J. J. Hope, Machine-designed sensor to make optimal use of entanglement-generating dynamics for quantum sensing, *Phys. Rev. Lett.* **124**, 060402 (2020).
- [69] J. Huang, M. Zhuang, J. Zhou, Y. Shen, and C. Lee, Quantum metrology assisted by machine learning, *Advanced Quantum Technologies* **n/a**, 2300329.
- [70] S. A. Haine, Using interaction-based readouts to approach the ultimate limit of detection-noise robustness for quantum-enhanced metrology in collective spin systems, *Phys. Rev. A* **98**, 030303 (2018).
- [71] K. A. Gilmore, M. Affolter, R. J. Lewis-Swan, D. Barberena, E. Jordan, A. M. Rey, and J. J. Bollinger, Quantum-enhanced sensing of displacements and electric fields with two-dimensional trapped-ion crystals, *Science* **373**, 673 (2021).
- [72] A. Browaeys and T. Lahaye, Many-body physics with individually controlled rydberg atoms, *Nature Physics* **16**, 132 (2020).
- [73] X. Wu, X. Liang, Y. Tian, F. Yang, C. Chen, Y.-C. Liu, M. K. Tey, and L. You, A concise review of rydberg atom based quantum computation and quantum simulation, *Chinese Physics B* **30**, 020305 (2021).
- [74] J. Ye and P. Zoller, Essay: Quantum sensing with atomic, molecular, and optical platforms for fundamental physics, *Phys. Rev. Lett.* **132**, 190001 (2024).